

A NEW CONCEPT FOR MIXED MODE FATIGUE CRACK GROWTH PREDICTIONS

W. Linnig*, H.A. Richard*

To be presented are the results of experimental investigations into the behaviour of fatigue cracks under a mixed mode fatigue load. Experiments carried out on CTS- and CCTS-specimens made from the aluminium alloy 7075-T651 show that crack extension in a new direction is the result of mixed mode loading on a Mode I fatigue precrack. In tests with constant stress intensity ΔK , it is possible to measure friction-induced decelerations in the crack growth that have yet to have been described by existing criteria. Furthermore, crack growth rates that are higher than those at the starter crack are to be measured after the phase of deceleration. In order to allow for the effects of deceleration, a mixed mode concept will be introduced as a complement to existing concepts.

INTRODUCTION

The investigation of fatigue crack growth under superimposed normal and shear loading represents an important field of fracture mechanics, the reason for this being that mixed mode loads frequently occur at the crack tip in practical situations as a result of the complex component and loading geometry. These combined loads are partly responsible for the changes in the direction and rate of crack growth. Fractographic analyses of actual damage reveal, for example, curved or zigzag-running fatigue cracks which are caused by the inherent stresses of the component or by alternating outer loads (Richard (1)).

A number of concepts already exist to describe crack growth under fatigue loads; these give the crack growth rate, respectively, as a function of the cyclic strain energy density ΔS_{\min} (Sih and Barthelemy (2)), as a function of the cyclic comparative stress intensity factor ΔK_v (Tanaka (3), Richard/Henn (4)), and as a function of the cyclic J-integral (Dai and Zheng (5)).

$$\frac{da}{dN} = C_1(\Delta S_{\min})^{m_1} = C_2(\Delta K_v)^{m_2} = C_3(\Delta J)^{m_3} \quad (1)$$

Experimental tests show, however, that a satisfactory prediction of the crack growth is not possible in certain cases. Having described the results of such experiments, we will then go on to present a new concept for the specification

* Institute of Applied Mechanics, University of Paderborn, FRG

of crack growth under mixed mode fatigue loading, a concept which is to be regarded as a complement to existing criteria.

EXPERIMENTAL INVESTIGATIONS

For the purpose of a more thorough investigation of the effect of Mode II and mixed mode loads on the growth behaviour of an actual Mode I fatigue crack, numerous experiments either with constant cyclic stress intensity factor ΔK or with constant outer load amplitude ΔP were conducted. Only those tests operating with constant ΔK will be dealt with here.

Preliminary tests

Whereas a crack continues to grow in the initial direction of extension under a pure Mode I load, a change of direction is brought about by applying a mixed mode load. With the aid of experimental pretests, it was possible to determine crack paths (Fig.2) that were dependent on the load parameters. These crack paths were used to produce FEM-meshes by means of which it was possible to calculate the stress intensity factors K_I and K_{II} . Using the fracture criteria of Richard (1), it is possible to calculate from the K_I - and K_{II} -values, the comparative stress intensity factor K_v

$$K_v = \frac{1}{2} K_I + \frac{1}{2} \sqrt{(K_I^2 + 6K_{II}^2)} \quad (2),$$

This, in its dimensionless form,

$$Y_v = Y_v \left(\frac{a}{W}, \alpha \right) = \frac{K_v}{\sigma \sqrt{\pi a}} = \frac{K_v}{\frac{P}{WB} \sqrt{\pi a}} \quad (3)$$

is used in the following tests to keep the stress intensity factor constant at the crack tip during the extension of the crack. Here W is specimen width, B specimen thickness, P outer load, and a the actual crack length.

Procedure und Material

The following experiments were carried out on CTS- and CCTS-specimens (Linnig et al (6)) in conjunction with the loading device developed by Richard (1). Only specimens with orientation T-L (in accordance with ASTM E399) were used. Their dimensions are given in Fig. 1. The typical properties measured for the aluminium alloy 7075-T651, the material used for the CCTS- and CTS-specimens, are:

Tensile yield stress	$\sigma_{YS} = 500 \text{ MPa}$
Ultimate tensile strength	$\sigma_{TS} = 582 \text{ MPa}$
Plane-strain fracture toughness	$K_{Ic} = 28.5 \text{ MPa}\sqrt{\text{m}}$

From a starter notch, a Mode I fatigue crack, length $a_1 = 54$ mm, is produced in the specimens. These are unloaded, rotated together with the loading device in a servohydraulic testing machine (loading angle $\alpha = 0^\circ$ (Mode I), $15^\circ, 30^\circ, \dots, 90^\circ$ (Mode II)) and thus subjected either to a mixed mode or a Mode II fatigue load.

In order to separate more effectively the parameters affecting the crack growth rates, the R-ratio ($R = 0.1, 0.3, 0.5$), the test frequency f ($f = 30$ Hz) and the cyclic stress intensity factor ΔK ($\Delta K = 7, 7.5, 8$ MPa $\sqrt{\text{m}}$) are kept constant throughout the experiments.

$$(\Delta K_I)_{\text{precrack}} = (\Delta K_V)_{\text{kinked crack}} = \Delta K = \text{konst.} \quad (4)$$

The necessary outer force amplitude ΔP calculated as follows

$$\Delta P = \frac{\Delta K_I W B}{\sqrt{\pi a} Y_I(a/W)} \quad \text{for the precrack} \quad (5)$$

$$\text{and } \Delta P = \frac{\Delta K_V W B}{\sqrt{\pi a} Y_V(a/W, \alpha)} \quad \text{for the kinked crack} \quad (6)$$

is set fully automatically on the tensile-testing machine. The crack length which needs to be known for the computation of the load amplitude is measured constantly with a DC potential drop method.

RESULTS

As a result of cyclic mixed mode loading, the crack paths that are formed after the change of load (Fig. 2) are dependent on the K_{II}/K_I -ratio. The angles of deflection φ_0 (Fig. 3) immediately after the kink are somewhat smaller for high K_{II}/K_I -ratios than is the case with static loading (see Richard (7)). The same angles of deflection (dependent on K_{II}/K_I) are to be measured for all R-ratios investigated; these may be described with the following approximation formula:

$$|\varphi_0| = 140^\circ \frac{|K_{II}|}{|K_I| + |K_{II}|} - 80^\circ \left[\frac{|K_{II}|}{|K_I| + |K_{II}|} \right]^2 \quad (7)$$

Consistent with the results from Mode I experiments, the crack growth rate of the kinked crack increases if either the amplitude of the stress intensity factor (Fig.4) or the R-ratio (Fig.5) is increased. Mean stress has no perceptible effect; the CTS- and CCTS- specimens yield the same crack growth rate in a Mode I crack where the same ΔK_I and the same R-ratio are present (Fig.4, Fig.6). This, although there is considerable divergence in the outer load amplitudes ΔP due to the different geometry functions Y (see Linnig et al (6)) of the two types of specimen.

Where the loading angle is large ($\alpha = 60^\circ, 75^\circ, 90^\circ$), a spontaneous decrease in the crack growth rate takes place immediately after the change of load – even though the stress intensity ΔK (calculated from the stress field) is kept

constant. After a particular crack length or a particular number of load cycles (this is dependent on the load parameters), the crack growth rate increases until a constant value is again reached. This value reaches or exceeds in the CTS-specimen the crack growth rate of the Mode I precrack (Fig. 5). An increase in the crack growth rate in correspondence to an increase in the K_{II}/K_I -ratio, such as Henn (4) describes for $R = 0.5$, was not to be observed with other R -ratios. The investigations that have so far been carried out on the CCTS-specimen (for only $\alpha = 45^\circ$, $R = 0.1$) display a different tendency. Only where high cyclic stress intensities ΔK_v are present does the crack growth rate approximately reach again the crack growth rate of the starter crack (Fig. 4).

The primary cause for the often marked changes in crack growth rate are the effects of friction on the flanks of the Mode I starter crack; these effects disappear either partially or completely again with the continued growth of the crack. The reason why the effects of friction are more noticeable in the CCTS-specimen than in the CTS-specimen (Fig. 4; Fig. 6) lies in their different geometry functions. Whereas, in the case of the CTS-specimen, the outer load amplitude needs to be increased after the load change in order to maintain a constant cyclic stress intensity ΔK_v , a decrease in the load is necessary for the CCTS-specimen. As a result, the effects of friction and therefore crack deceleration are intensified.

Similar deceleration effects are to be observed in tests where the outer load amplitude ΔP is constant (see Linnig (6)).

LIFETIME PREDICTION OF KINKED CRACKS

Further experiments and investigations with an electron scan microscope have shown that it is the effect of friction on the flanks of a Mode I starter crack that is responsible for the reduction in the effective stress intensity and therefore in the crack growth rate during the development phase of a kinked crack. As well as the plasticity- and oxide-induced closure (fretting oxidation mechanism), the roughness-induced closure also plays an important part during this phase; an effect similar to that on the crack extension near the threshold range is to be observed. So far it has not been possible to reduce to a formula, these mechanisms which are dependent on both the test parameters and the material-specific properties. We have developed a mixed mode concept, the underlying idea which is as follows: to describe, where possible, crack growth rates with the known Mode I and mixed mode concepts and to estimate the transition zones caused by the kinking of the crack with the aid of the transition load cycles N_t and the transition crack length a_t . The latter are found by experiment. For a kinked crack which has grown first under a Mode I and then under a mixed mode load (Fig 6), for instance, the total number of load cycles N is calculated as follows:

$$N = N_I + N_t + N_{mm} \quad (8).$$

The number of load cycles N_I is obtained by integrating, for example, the PARIS equation, the number of load cycles N_{mm} by the integration of a

modified PARIS equation (see HENN (4)). The number of load cycles N_t is derived from the nomogram to be described below. Similarly, for the total crack length a after a random number of load cycles N :

$$a = a_i + a_t + a_{mm} \quad (9).$$

In order to specify the transition crack length a_t and transition load cycles N_t , experiments carried out with constant outer load amplitude ΔP and with constant cyclic stress intensity ΔK are analysed. For the evaluation of the tests with ΔK constant, the transition zone is defined as the zone between the load change and the return to a constant crack growth rate (Fig.6). The analysis of the tests with ΔP constant (these tests are not described here) requires, however, a complicated definition of the transition zone in some cases; the definition depends on whether the stress intensity is increased or reduced through the change of load.

With the aid of the definition for the transition range, it is possible to determine the values of a_t and N_t from the da/dN - a -diagram (Fig. 6) and the da/dN - N -diagram (Fig. 7).

The values of a_t and N_t may be represented in the form of a nomogram (Fig.8); this permits a_t and N_t to be determined as functions of the K_{II}/K_I -ratio, the R -ratio, the amplitude of the stress intensity immediately before the change of load, and the T -ratio. The T -ratio $T = \Delta K_{mm}/\Delta K_I$ takes care of the change in the stress intensity due to the change of load ($T = 1$ in tests with $\Delta K = \Delta K_I = \Delta K_{mm} = \text{const.}$).

The nomogram consists of 5 squares; these allow for the various test parameters. For a constant $\Delta K_I = \Delta K_v = 7\text{MPa}\sqrt{\text{m}}$, the transition load cycles N_t and the transition crack length a_t are shown as a function of the R -ratio in the middle square of the top row. Allowance is made for the effect of the other test parameters on the transition zone in the two lefthand squares for N_t and in the two righthand squares for a_t , respectively. By starting, as shown in Fig.8, from the $K_{II}/(K_I+K_{II})$ -ratio and going round the nomograph once anticlockwise ($\rightarrow N_t$) and once clockwise ($\rightarrow a_t$), it is possible to determine the values N and a .

Knowing N_t and a_t , the transition zone may be estimated and given due consideration in a calculation of the time-to-failure.

ACKNOWLEDGEMENT

The authors wish to thank the Deutsche Forschungsgemeinschaft (DFG) – German Research Association – for its financial support.

REFERENCES

- (1) Richard, H.A., "Bruchvorhersagen bei überlagerter Normal- und Schubbeanspruchung sowie reiner Schubbeanspruchung von Rissen", VDI-Forschungsheft 631, Düsseldorf, 1985
- (2) Sih, G.C. and Barthelemy, B.M., Engng. Fract. Mechanics, Vol. 13, 1980, pp. 439-451
- (3) Tanaka, K., Engng. Fract. Mechanics, Vol. 6, 1974, pp. 493-501
- (4) Henn, K., Richard, H.A., Linnig, W., "Fatigue crack growth under mixed mode and mode II cyclic loading", in: Failure Analysis - Theory and Practice (ECF 7), ed. by E. Czoboly, EMAS, Hungary, 1988, pp. 1104-1113
- (5) Dai, Y. and Zheng, G.H., "On fatigue crack growth under mixed mode cyclic loading", in: Numerical Methods in Fracture Mechanics, ed. by A.R. Luxmoore et al., pp. 669-676
- (6) Linnig, W., Richard, H.A., Henn, K., "Change in the crack growth rates under mixed mode loading", Proceedings of the Intern. Conf. Fatigue 90, Honolulu, 1990
- (7) Richard, H.A., "Mixed mode fracture and fatigue processes", in: Applied Mechanics, ed. by Zheng Zhemin, ICAM 1989, pp. 1837-1842

FIGURES

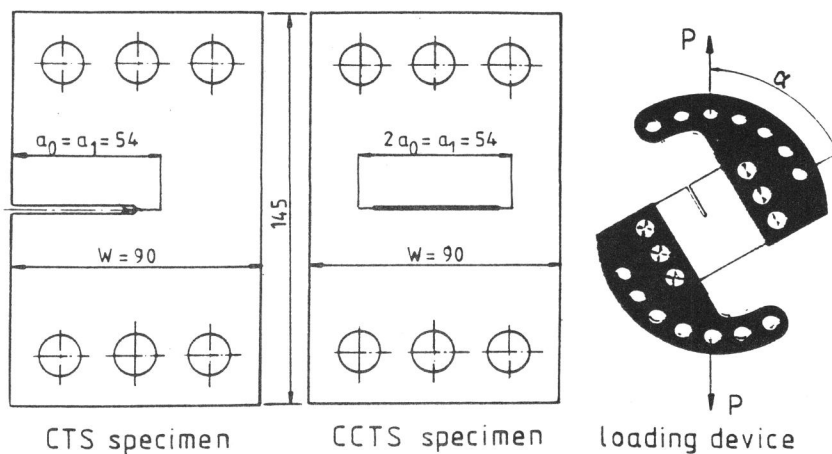


Fig. 1 CTS- and CCTS-specimen for generation of Mode I, Mode II, and mixed mode loading of the crack, and the special loading device

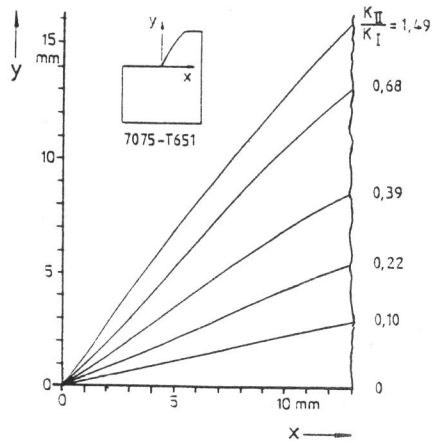


Fig. 2 Crack paths in CTS-specimens

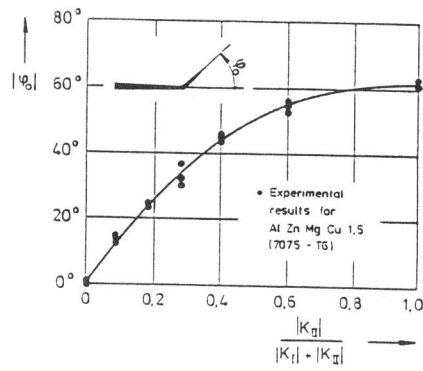


Fig. 3 Crack deflection angle measured for 7075-T651

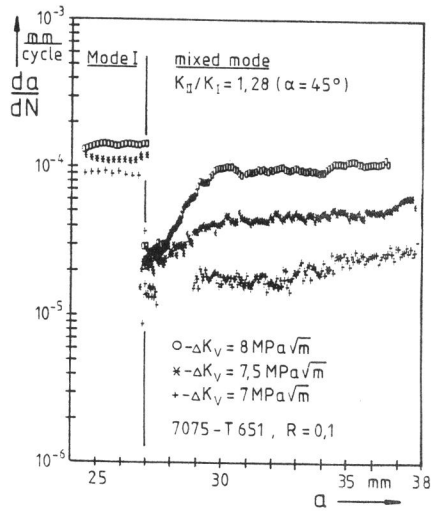


Fig. 4 Comparison of tests with ΔK const. (CTS-specimen)

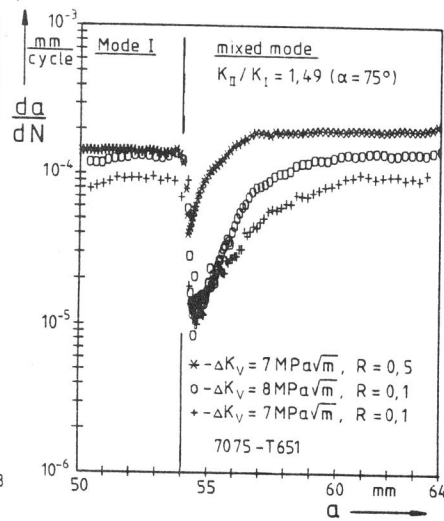


Fig. 5 Effect of R-ratio on crack growth rate

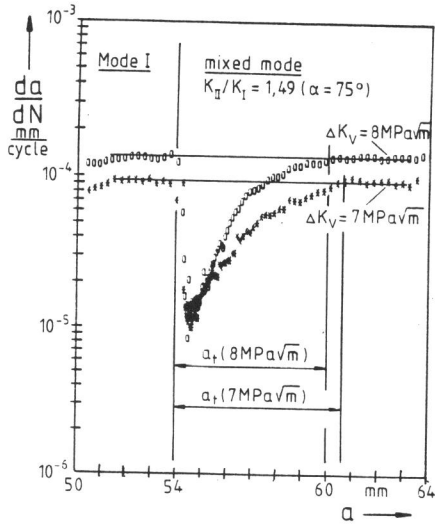


Fig. 6 Transition crack length a_t ($\Delta K = \text{const.}, \text{CTS-specimen}$)

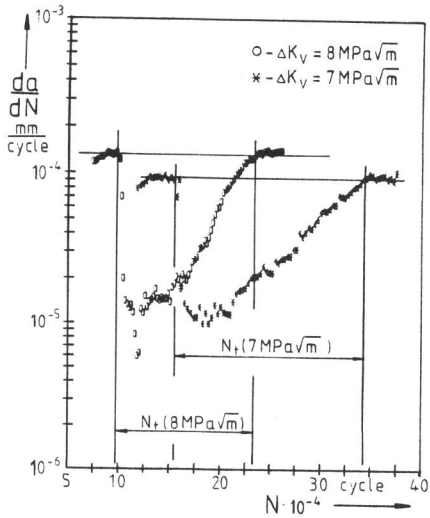


Fig. 7 Transition load cycles N_t ($\Delta K = \text{const.}, \text{CTS-specimen}$)

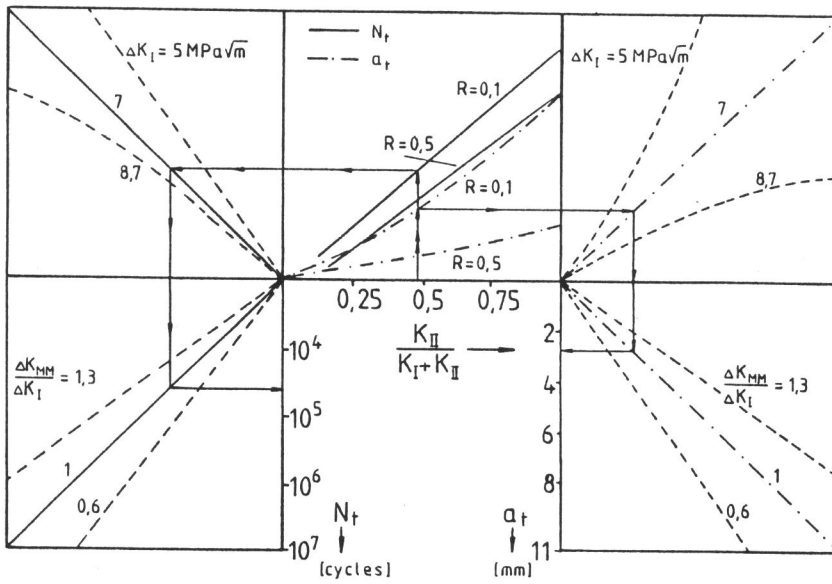


Fig. 8 Nomogram for the specification of the transition crack length a_t and the transition load cycles N_t after a sudden change of load on the aluminium alloy 7075-T651